International Journal of Fluid Power 9 (2008) No. 1 pp. 17-26

DESIGN AND ANALYSIS OF A TWO-STAGE POPPET VALVE FOR FLOW CONTROL

Matthew T. Muller[1] and Roger C. Fales[2]

[1]*Caterpillar Inc. – Technology and Solutions Division – Hydraulics Research, Peoria, IL, USA*
[2]*University of Missouri - Columbia, Mechanical and Aerospace Engineering, Columbia, MO 65211, USA*
Muller_Matt@cat.com, FalesR@missouri.edu

Abstract

This paper explores dynamic modelling and design of a typical two stage metering poppet valve system. In particular, nonlinear and linear models of a spring force feedback configuration are developed and parameters tuned through the use of root locus techniques. Typical steady state conditions as well as extreme high and low pressure drops are simulated in attempts to uncover instabilities and other possible undesirable performance characteristics of the valve. Finally the nonlinear model is used to produce Bode magnitude plots at various pressure drops in order to estimate the system bandwidth. Results indicate that increasing the size of the orifice at the inlet of the pilot stage of the valve increases performance in terms of rise time at the cost of a more oscillatory response. High pressure differences between the inlet and outlet of the valve were found to cause performance to increase significantly as well as move poles into a region indicated less damping. A scheme for controlling the inlet orifice area to the pilot stage is presented and shown to improve performance capability (bandwidth) of the valve while maintain a damped response.

Keywords: metering poppet valve, root locus design, valve design

1 Introduction

Electro-hydraulic control valves are extensively used in industry to control motion in various devices. For many years the standard has been to use spool type valves along with separate supply pressures for the pilot and main stages of flow. Poppet valves have been available for many years but have been limited in use to situations such as pressure relief. Over the past ten years there has been a push to develop poppet valves that can meter flow in the way spool valves have typically been used (Zhang et al., 2002), (Schexnayder, 1995), (Aardema, 1997), (Yang et al., 1997), (Yang et al., 2005), (Fales, 2006). The incentives behind this growing trend are the advantages that come with the use of poppet valves. In comparison to spool valves, poppet valves require less stringent machining tolerances, are less susceptible to contamination problems, have very low leakage, and make it possible to eliminate two separate supply lines (Manring, 2005). Although poppet valves present many advantages to spool valves they have yet to take over the market due to a long history of instability issues. The unstable behavior in poppet valve circuits have been studied by Hayashi (1995) , Funk (1964), and others but there is still no clear path to avoiding this problem. In recent years there have been metering poppet valves that have proved successful enough to become commercially available. Zhang et al. (2002) study the dynamics of one such valve and suggest performance limitations due to zero location. Opdenbosch et al. (2004) models a newer poppet valve with a position follower configuration and proposes a controller based on a Nodal Link Perceptron Network. The list of papers in the open literature related to modeling the dynamics of metering poppet valves surrounds the few commercially produced valves but there is little to no focus in the literature providing guiding techniques for designing a metering poppet valve from a ground up approach. Although the literature is scarce in regards to the design of metering poppet valves, existing research provides design methods which can be applied to poppet valves. One such example comes from Li (2002), who uses root locus analysis to redesign a two-spool flow control servo valve. The goals of this research are to use root locus techniques and frequency response plots com-

This manuscript was received on 2 October 2007 and was accepted after revision for publication on 3 February 2008

bined with nonlinear simulations in attempts to design a novel poppet valve that can accurately meter flow while maintaining a bandwidth, defined as a 3dB drop from the low frequency gain or 0.707 of the low frequency gain in absolute terms, of 8 Hertz or greater.

The models developed in this paper are for a two stage electro-hydraulic poppet valve that is arranged in a forced feedback setup as shown in Fig.1. The valve is currently under development at the University of Missouri – Columbia.

The following paragraph gives a brief description of the operation of the metering poppet valve design. With respect to Fig. 1, the valve is in the closed position with high pressure connected to the inlet port {3} while low pressure is connected to the outlet port {1}. The only two pathways from high to low pressure are sealed by poppet seats and therefore the valve maintains a very low leak. It is assumed that the pilot poppet {9} is pressure balanced by appropriate means while being subjected to the actuator's force {10}, the feedback spring's force {6}, viscous damping, and flow forces. In order to raise the main poppet {4} off its seat, a pulse width modulated signal (PWM) signal supplies current to the actuator solenoid which pushes the pilot poppet off its seat and allows fluid to exit the control volume {7} through its outlet orifice {8}. Once the pilot poppet opens, the control volume inlet orifice {5} is effectively smaller than its outlet orifice creating a net outflow which allows the main poppet to lift off its seat. This opens an orifice {2} directly between supply and load, allowing flow to be metered. The upward movement of the main poppet will push the feedback spring and in turn push the pilot poppet back towards its seat until an equilibrium position is reached where the main poppet is open yet no longer moving. In order to close the main poppet, the actuator current is turned off allowing the feedback spring to push the pilot poppet back to its seat. The control volume outlet orifice is now closed while high pressure fluid from the inlet orifice fills the control volume and pushes the main poppet closed.

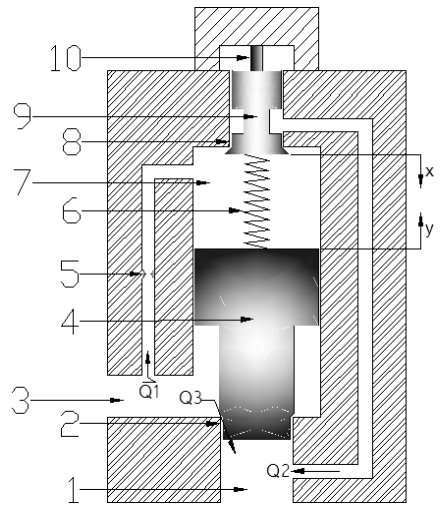

Fig. 1: *Force Feedback Poppet Configuration*

The paper is organized as follows: the general mathematical model is presented, analysis of the model through root locus techniques and Bode plots follows, an alternative model is proposed and analyzed, and finally conclusions are presented.

2 Mathematical Model

Initial equations were derived to model the dynamics embodied in Fig. 1 while geometry was chosen in attempts to produce a flow of 120 LPM with the main poppet fully open and a pressure drop of 2.1 MPa. The initial model parameters were chosen with the understanding that further analysis presented later in this work would be used to modify them.

The general model can be broken into four basic systems or governing equations: two spring mass damper systems with flow and pressure forces for each poppet, a pressure rise rate equation for the control volume, and a pressure rise rate equation for the load volume. The forces acting on the main poppet are represented by Eq. (1).

$$M\ddot{y} = -b_y\dot{y} - k(y+x) - P_c A_c + P_s A_s + P_L A_L - 2\cos(\theta)C_d^2 h_3 y(P_s - P_L) \quad (1)$$

The preload force due to the spring asymbled between the pilot and main poppets is considered small by design. It is noted that the last term in Eq. 1 represents the flow forces on the poppet and that in general flow forces in this paper will be considered to act in a direction such as to restrict the given orifice (move the poppet in a direction which closes the orifice). It is also noted that the coefficient on the flow force term, two times the cosine of the jet angle, θ, is highly affected by the choice of jet angle. In this case 55 degrees is the estimate of the jet angle which is equal to the half conic angle of the poppet valve.

The forces acting on the pilot poppet are represented by Eq. 2, with '*f*' representing the input force from the actuator. Again, it is noted that no pressure terms appear in Eq. 2 because the pilot poppet is considered pressure balanced. Although the pilot poppet is subject to nonlinear damping forces the model is simplified by accounting for these forces by increasing the linear damping coefficient.

$$m\ddot{x} = -b_x\dot{x} - k(y+x) + f - 2\cos(\theta)C_d^2 h_2 x(P_c - P_L) \quad (2)$$

The change in control volume pressure is given by Eq. 3. A linear version of the pressure rise rate equation has been used here and in models to follow. The assumption has been made that volume change as a result of poppet movement is small compared to the nominal control volume and therefore control volume is considered constant. This is generally true due to poppet valves having very short displacements. It is also noted that the effect on $\dot{P}_c$ from $\dot{x}$ has been neglected due to the relatively small area and displacement of the pilot poppet as compared to the main poppet.

$$\dot{P}_c = \frac{\beta}{V_{CO}}(Q_1 - Q_2 + A_c\dot{y}) \quad (3)$$

The change in load volume pressure is given by Eq. 4. For all models except those with constant load

pressure, load is represented by a fixed volume followed by an orifice to a constant tank pressure. In order to simulate different conditions, the area of the load orifice is varied as needed.

$$\dot{P}_{\mathrm{L}} = \frac{\beta}{V_{\mathrm{L}}}(Q_2 + Q_3 - Q_4) \tag{4}$$

The flow terms, Q_1-Q_4, in Eq. 3 and Eq. 4 are modeled using the classic orifice equation.

$$Q = aC_{\mathrm{d}}\sqrt{\tfrac{2}{\rho}\Delta P} \tag{5}$$

In cases where an orifice is variable its area is equivalent to the slope of the orifice '*h*' multiplied by the position of the poppet which creates the orifice.

Equations 1 to 5 represent a nonlinear model of the forced feedback poppet as shown in Fig. 1. Although the nonlinear model is more appropriate for examining valve behavior and frequency response, a linear simplification and accompanying tools provide better information as to which parameters should be tuned to improve system performance. In order to achieve a linear model, the flow force terms, which are dependent on both pressure and position, and the orifice equation, which depends on position and the square root of pressure, are linearized about a nominal valve position. Through Taylor series expansion, the flow force terms of Eq. 1 and Eq. 2 can in general be approximated by Eq. 6.

$$\begin{aligned} &flowforce = (2\cos(\theta)C_{\mathrm{d}}^2 a_{\mathrm{O}})\Delta P + \\ &\qquad (2\cos(\theta)C_{\mathrm{d}}^2 h\Delta P_{\mathrm{O}})displacement \\ &or \quad flowforce = kfc \times \Delta P + kfq \times displacement \end{aligned} \tag{6}$$

It is noted that *displacement* represents the distance the poppet has moved from its nominal position while a_{O} and P_{O} represent conditions while the valve is at the nominal position. A Taylor series expansion of the classic orifice equation results in the linear approximation shown in Eq. 7.

$$\begin{aligned} &Q = Q_{\mathrm{O}} + \left(\frac{a_{\mathrm{O}}C_{\mathrm{d}}}{\sqrt{2\rho\Delta P_{\mathrm{O}}}}\right) \times \Delta P + \left(hC_{\mathrm{d}}\sqrt{\tfrac{2}{\rho}\Delta P_{\mathrm{O}}}\right) \times displacement \\ &or \quad Q = Q_{\mathrm{O}} + kc \times \Delta P + kq \times displacement \end{aligned} \tag{7}$$

Substituting appropriate linearizations into Eq. 1 to 4 the linear model is then represented by Eq. 8 to 11 with initial conditions removed. The states become perturbations from nominal conditions.

$$\begin{aligned} M\ddot{y} = &-b_y\dot{y} - k(y_{\mathrm{n}} + x_{\mathrm{n}}) - kfq_3 y_{\mathrm{n}} - \\ &kfc_3(P_s - P_{\mathrm{L}}) - P_{\mathrm{c}}A_{\mathrm{c}} + P_{\mathrm{s}}A_{\mathrm{s}} + P_{\mathrm{L}}A_{\mathrm{L}} \end{aligned} \tag{8}$$

$$\begin{aligned} m\ddot{x} = &-b_{\mathrm{x}}\dot{x} - k(y_{\mathrm{n}} + x_{\mathrm{n}}) + \\ &f - kfc_2(P_c - P_{\mathrm{L}}) - kfq_2 x_{\mathrm{n}} \end{aligned} \tag{9}$$

$$\begin{aligned} \dot{P}_{\mathrm{c}} = &\frac{\beta}{V_{\mathrm{Co}}}\{kc_1(P_{\mathrm{s}} - P_{\mathrm{c}}) - kq_2 x_{\mathrm{n}} \\ &- kc_2(P_{\mathrm{c}} - P_{\mathrm{L}}) + A_{\mathrm{c}}\dot{y}\} \end{aligned} \tag{10}$$

$$\begin{aligned} \dot{P}_{\mathrm{L}} = &\frac{\beta}{V_{\mathrm{L}}}\{kq_2 x_{\mathrm{n}} + kc_2(P_{\mathrm{c}} - P_{\mathrm{L}}) + kq_3 y_{\mathrm{n}} + \\ &kc_3(P_{\mathrm{s}} - P_{\mathrm{L}}) - kc_4(P_{\mathrm{L}} - P_{\mathrm{T}})\} \end{aligned} \tag{11}$$

After choosing geometry, establishing a spring constant, and determining supply and tank pressures it is possible to calculate nominal pressures and hence to calculate the coefficients needed for the linear flow and flow force equations. Under nominal conditions the main poppet only has static forces acting on it and hence, neglecting flow forces, Eq. 1 reduces to:

$$P_{\mathrm{CO}} = \begin{pmatrix} P_{\mathrm{s}}A_{\mathrm{s}} + P_{\mathrm{LO}}A_{\mathrm{L}} - k(x_{\mathrm{O}} + y_{\mathrm{O}}) - \\ 2\cos(\theta)C_{\mathrm{d}}^2 h_3 y(P_{\mathrm{s}} - P_{\mathrm{LO}}) \end{pmatrix}\frac{1}{A_{\mathrm{c}}} \tag{12}$$

Equation 2 reduces to Eq. 13 where f is an arbitrary input to be chosen depending on the nominal position one wishes to study.

$$\begin{aligned} f = &k(x_{\mathrm{O}} + y_{\mathrm{O}}) + \\ &2\cos(\theta)C_{\mathrm{d}}^2 h_2 x(P_{\mathrm{cO}} - P_{\mathrm{LO}}) \end{aligned} \tag{13}$$

Static equilibrium of the each poppet also dictates that flow in must equal flow out. Examining the control volume gives $Q_1 = Q_2$, which after simplification becomes:

$$P_{\mathrm{LO}} = P_{\mathrm{cO}} - \left(\frac{a_{1\mathrm{fix}}}{a_{2\mathrm{O}}}\right)^2 (P_{\mathrm{s}} - P_{\mathrm{cO}}) \tag{14}$$

Examining the load orifice gives $Q_2 + Q_3 = Q_4$, which after simplification becomes:

$$P_{\mathrm{LO}} = \frac{{a_2}^2 P_{\mathrm{cO}} + {a_{3\mathrm{O}}}^2 P_{\mathrm{s}} + a_{4\mathrm{fix}}^2 P_{\mathrm{T}}}{a_{2\mathrm{O}}^2 + a_{3\mathrm{O}}^2 + a_{4\mathrm{fix}}^2} \tag{15}$$

Given that $a_{2\mathrm{O}} = x_{\mathrm{O}}h_2$ and $a_{3\mathrm{O}} = y_{\mathrm{O}}h_3$ there are only four unknowns, (P_{CO}, P_{LO}, x_{O}, y_{O}), allowing Eq. 12 to 15 to be solved and the coefficients for the linear model to be determined.

3 Model Analysis

Although the above linearization requires geometry to be established, a goal of this research is to use linear design tools to select geometry and other parameters that will enhance stability and performance. In order to achieve this, an iterative procedure is utilized in which an initial linear model is created and root locus plots serve as a guide to improving valve parameters. The preliminary model is developed from flow requirements, basic physics, and an array of nonlinear simulations until functional linearizations and root locus plots are created. Root locus plots for various parameters, valve openings, and pressure drops must be examined together and then a decision is made on which parameter(s) to change in attempts to optimize the stability, speed of response, and damping of the system. After a parameter is changed, results can be examined with nonlinear simulations and new linearizations can be created. New linearizations give rise to a new set of root locus plots and the procedure is repeated until valve performance meets necessary objectives as dictated by results from nonlinear simulations.

To begin the iterative procedure Eq. 8 to 11 are written in state space form, as shown in Eq. 16, and

employed to generate root locus plots for desired parameters.

$$z_1 = y_n \quad z_2 = \dot{y} \quad z_3 = x_n \quad z_4 = \dot{x} \quad z_5 = P_L \quad z_6 = P_c$$

$$\begin{pmatrix} 0 & 1 & 0 & 0 & 0 & 0 \\ \frac{(-k-kfq_3)}{M} & \frac{-b_y}{M} & \frac{-k}{M} & 0 & \frac{(kfc_3+A_L)}{M} & \frac{-A_c}{M} \\ 0 & 0 & 0 & 1 & 0 & 0 \\ \frac{-k}{m} & 0 & \frac{(-k-kfq_2)}{m} & \frac{-b_x}{m} & \frac{kfc_2}{m} & \frac{-kfc_2}{m} \\ \frac{\beta}{V_L}kq_3 & 0 & \frac{\beta}{V_L}kq_2 & 0 & \frac{-\beta}{V_L}(kc_2+kc_3+kc_4) & \frac{\beta}{V_L}kc_2 \\ 0 & \frac{\beta}{V_{co}}A_c & \frac{-\beta}{V_{co}}(kq_2) & 0 & \frac{\beta}{V_{co}}kc_2 & \frac{-\beta}{V_{co}}(kc_1+kc_2) \end{pmatrix} \begin{pmatrix} z_1 \\ z_2 \\ z_3 \\ z_4 \\ z_5 \\ z_6 \end{pmatrix} +$$

$$\begin{pmatrix} 0 \\ \frac{-k(x_o+y_o)+(-kfc_3+A_s)P_s}{M} \\ 0 \\ \frac{f-k(x_o+y_o)}{m} \\ \frac{\beta}{V_L}\left[kc_3P_s+kc_4P_T+Q_{2O}+Q_{3O}-Q_{4O}\right] \\ \frac{\beta}{V_{co}}\left[kc_1P_s+Q_{1O}-Q_{2O}\right] \end{pmatrix} = \begin{pmatrix} \dot{z}_1 \\ \dot{z}_2 \\ \dot{z}_3 \\ \dot{z}_4 \\ \dot{z}_5 \\ \dot{z}_6 \end{pmatrix} \tag{16}$$

A program is written that calculates the eigenvalues or roots of the state transition matrix while one parameter is varied within a loop. In particular, root locus plots are examined for the area of orifice one, the slopes for orifice two and three, the spring rate, and the damping coefficient on the pilot poppet. It is thought that poppet valve instabilities often arise when the main poppet is just cracked open and hence the bulk of linearizations are for conditions in which the main poppet is open to 25 % of the maximum opening or less. In an attempt to uncover various performance problems with the valve, separate linearizations are created for different pressure scenarios including:

$$(P_s = 35MPa \quad \Delta P \approx 35MPa),$$
$$(P_s = 35MPa, \Delta P \approx 1MPa),$$
$$(P_s = 21MPa, \Delta P \approx 2.1MPa), \text{ and}$$
$$(P_s = 2.1MPa, \Delta P \approx 1MPa)$$

where $\Delta P = P_S - P_L$ Fig. 2 to 7 show root locus plots for linearizations where the input force to the pilot poppet is 8 % of the maximum possible force and the pressure drop across the valve is approximately 2.1 MPa. The root locus moves towards the *X* with a triangle around it as the parameter value is increased. Arrows are drawn on the figures to clarify the direction in which the roots are moving as the parameters vary. In Fig. 5 to 7 the two poles to the far left, which appear in Fig. 4, have been excluded as they are relatively stationary and their removal significantly improves graph readability.

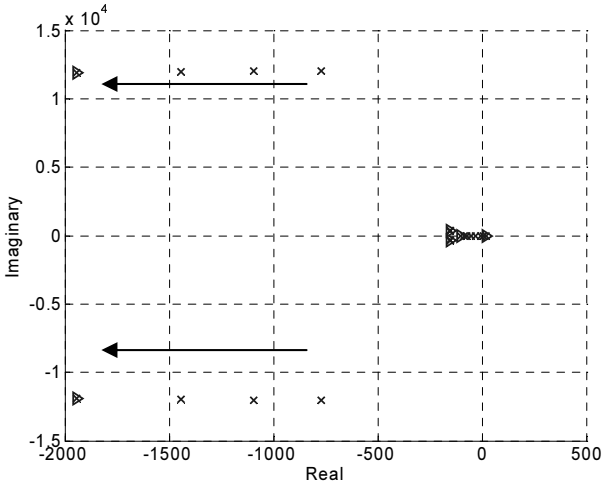

Fig. 2: *Root locus varying a_1 (P_S = 21 MPa, $\Delta P \approx 2.1$ MPa)*

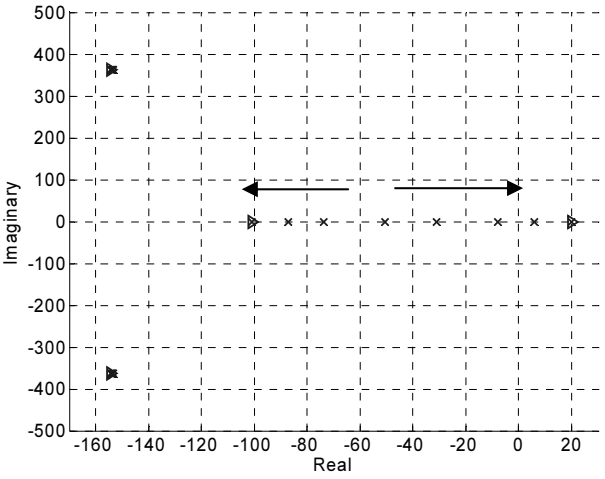

Fig. 3: *Zoom of the right portion of Figure 2.*

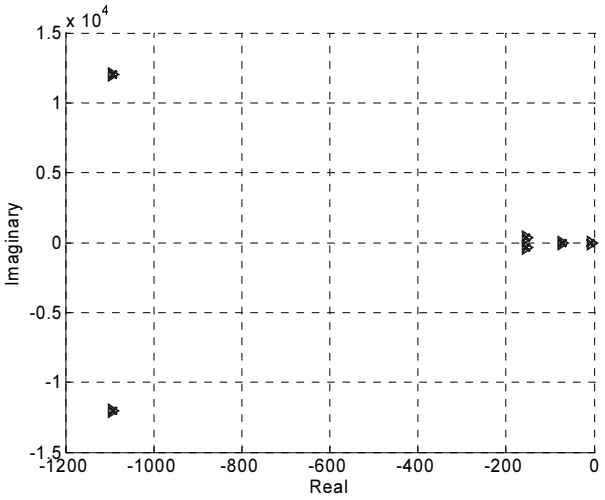

Fig. 4: *Root locus varying h_3: P_S = 21 MPa, $\Delta P \approx 2.1$ MPa*

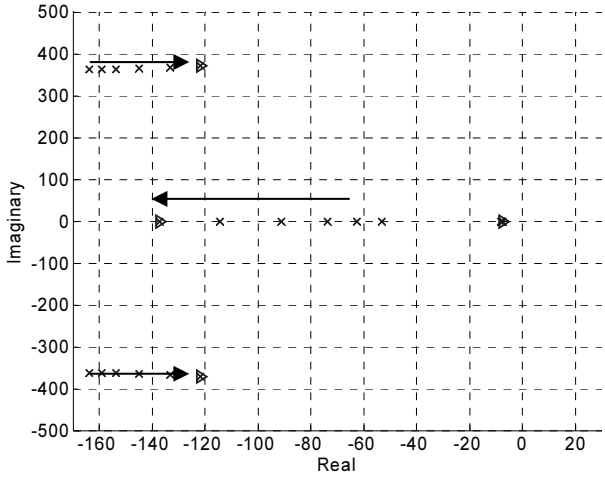

Fig. 5: *Root locus varying h_2: P_S = 21 MPa, $\Delta P \approx 2.1$ MPa*

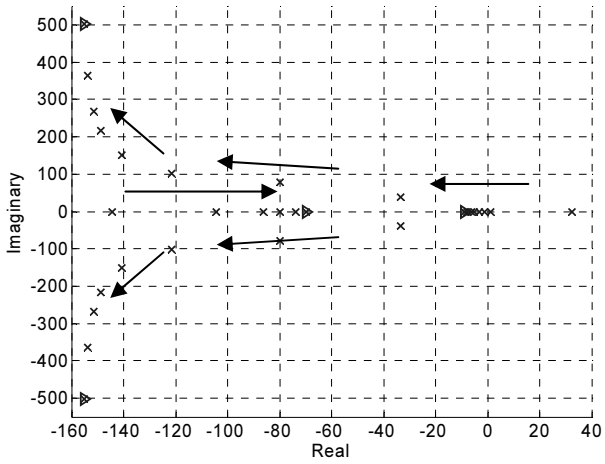

Fig. 6: *Root locus varying k (spring rate): P_S = 21 MPa, $\Delta P \approx 2.1$ MPa*

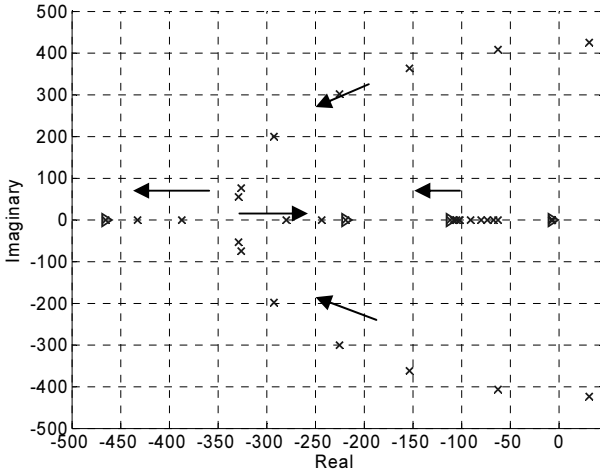

Fig. 7: *Root locus varying b_X (pilot damping): P_S = 21 MPa, $\Delta P \approx 2.1$ MPa)*

Figures 2 and 3 demonstrate that of the parameters examined, a variation in a_1 has the greatest impact on the position of the two left most poles as well as the right most pole. Figure 4 shows that the slope of the main poppet orifice may have little impact on the systems poles while Fig. 5 establishes a connection between the slope of the pilot orifice and system oscillation. Figure 6 reveals that if the spring rate is too low the valve will be unstable while if it is too high excessive oscillation can occur. Finally, Fig. 7 displays a correlation between the damping of the pilot poppet and the damping of the entire system. Caution is taken in making claims on valve performance based on Fig. 2 to 7 due to the fact these root locus plots originate from just one operating point. There is no reason to assume the valve will behave the same under more extreme pressure drops or larger nominal openings due to nonlinearity. Because of the large number of root locus plots needed to examine the valve in various scenarios, only a select few will be shown to demonstrate contrasting information to what it shown in Fig. 2 to 7.

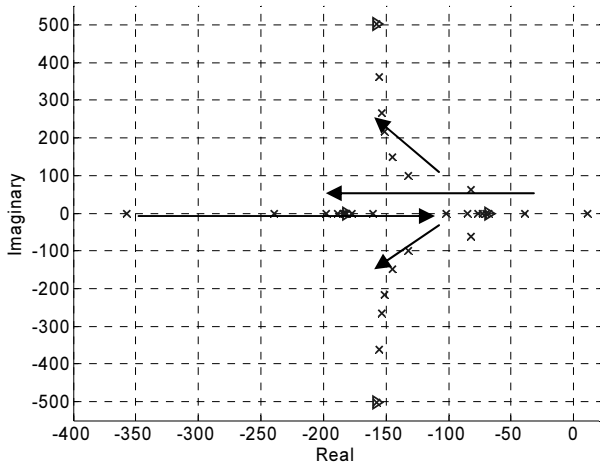

Fig. 8: *Root locus varying k (30 N input): P_S = 21 MPa, $\Delta P \approx 2.1$ MPa*

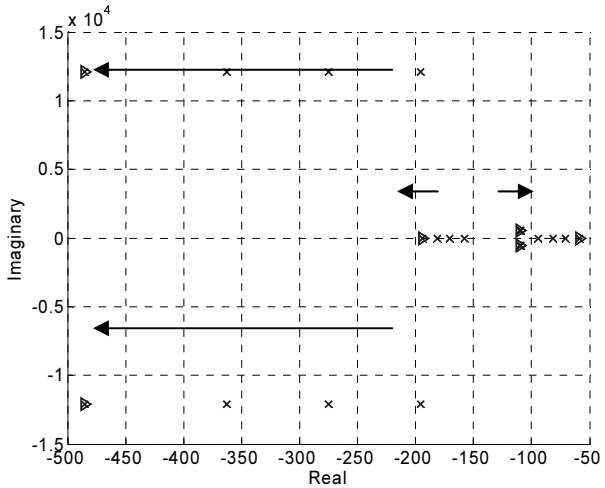

Fig. 9: *Root locus varying a_1: P_S = 35 MPa, $\Delta P \approx 35$ MPa*

Careful examination of the root locus plots from various valve openings and pressure drops reveals that the complex roots and the left most real root, as seen in Fig. 2 to 7, appear almost identical for different valve openings (different force inputs) when the pressure drop is held constant. Figure 8 supports this statement by displaying similar root movement to that of Fig. 6 even though the valve is now open 3.5 mm instead of 0.5 mm. It should be noted that the root locus path clustered around -10 in Fig. 6 has shifted to the left and ends at approximately -180 radians per second in Fig. 8.

Although five of the six roots appear nearly independent of valve position they shift dramatically and even take different shape as the pressure drop is varied. Figure 9 is a root locus plot for the scenario depicted in Figs. 2 and 3 with the only change being an increase in pressure drop form 2.1 MPa to 35 MPa. Comparing these figures, one can see that an increase in pressure drop results in a dramatic shift of all root locus paths.

Figure 10 can be contrasted with Fig. 6 and demonstrates different behavior as the spring constant is increased. Both figures link a higher spring rate to more oscillation. Figure 10 shows that high spring rates tend to cause a less damped behavior for the low pressure case due to the complex pole locations. Figure 10 also makes it clear that some of the poles are moving in different directions than in the case with a lower pressure drop.

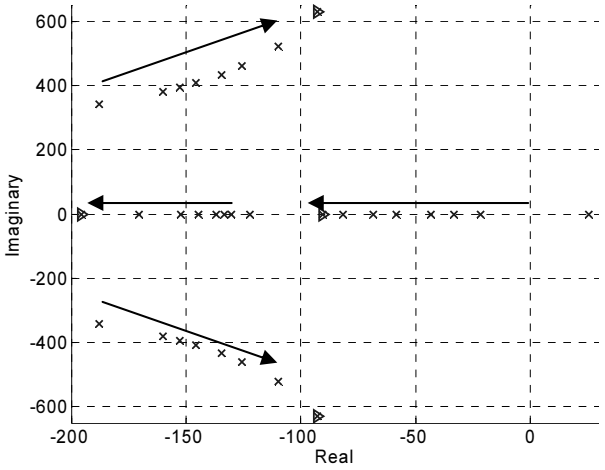

Fig. 10: *Root locus varying k: P_S = 35 MPa, $\Delta P \approx 35$ MPa*

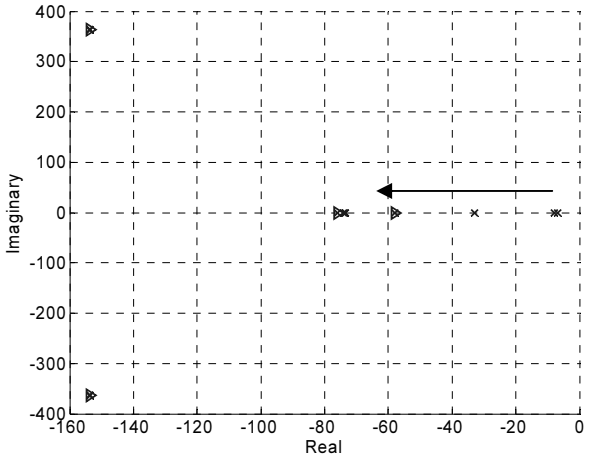

Fig. 11: *Root locus varying kc_4: P_S = 21 MPa, $\Delta P \approx 2.1$ MPa*

The real root that is located at approximately -10 in Fig. 2 to 7 shifts in Fig. 8 to 10 but not in a way that is easily predictable with pressure drop. A thorough examination of its movements reveals that it is the pole which reflects load dynamics or the fifth state equation. Figure 11 brings light to the dominant effect kc_4 (pressure flow coefficient for the load orifice) has on the location of this pole. In Fig. 11 the right most pole moves from -10 to -63 as kc_4 increases.

Although the root at -10 in Figs. 2-7 appears to make the system unacceptably slow, Fig. 11. suggests this may not be the case. kc_4 is dependent on the load orifice area which has been arbitrarily adjusted to achieve desired pressure drops across the valve. The impact that kc_4 or the entire fifth state equation has on the system dynamics is also dependent on V_L (load volume) which again is an arbitrary value. Due to these limitations of the model, caution should be taken when interpreting the relationship between load dynamics and valve performance.

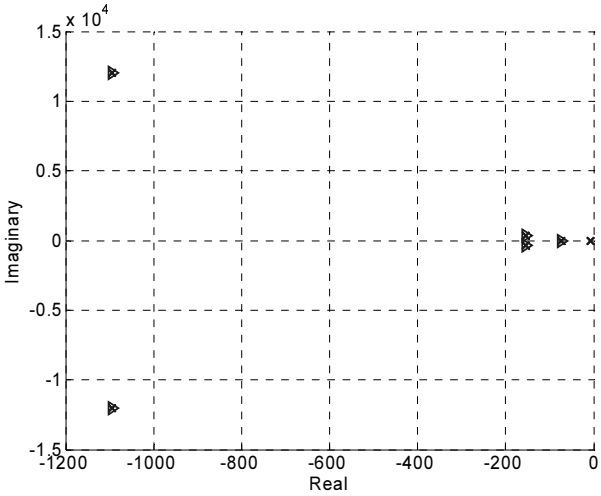

Fig. 12: *Final System Roots: P_S = 21 MPa, $\Delta P \approx 2.1$ MPa*

The information attained from the root locus plots provides evidence as to which design constraints will have the most impact on system stability and performance. Parameters surrounding the entrance and exit orifices to the control volume and the feedback spring come directly from the root locus analysis as well as verification from nonlinear simulations. The final values for pilot damping and the slope of main poppet orifice are connected to damping measurements from existing valves and from the desired 120 LPM flow rate. Figure 12 displays the roots for the final system corresponding to scenario presented in Fig. 2 to 7. The root that is not enclosed by a triangle represents the load pressure rise rate equation. When load pressure is held constant the poles for the system become the triangles in Fig. 12.

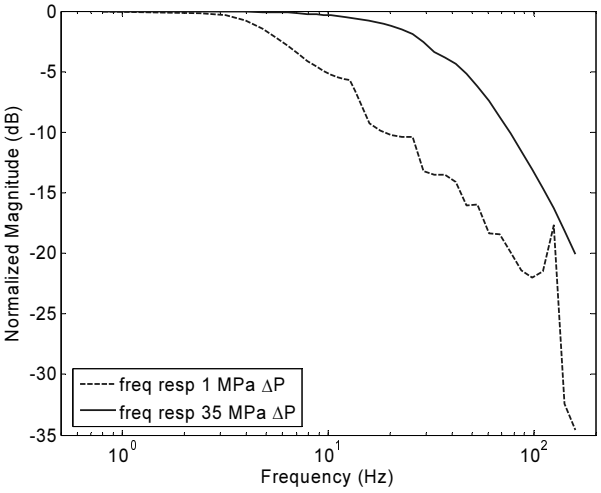

Fig. 13: *Bode diagram from nonlinear simulations*

Due to the realized limitations of the above load model the following Bode diagram is for the nonlinear system when load pressure is held constant. The Bode diagram appearing in Fig. 13 is for the main poppet position, where the solenoid input force is a sinusoid such that the low frequency amplitude is 50 % of the maximum poppet stroke. The system bandwidth is approximately 32Hz for a 35 MPa pressure drop across the valve and 6.5 Hz for a 1 MPa pressure drop.

It is noted that according to Fig. 13, the design criteria set forth in the introduction have not been met for pressure drops as low as 1 MPa. Nonlinear simulations suggest that if a bandwidth of 8 Hz is to be achieved for this pressure drop, alternative designs should be considered. A time response of main poppet position of the metering poppet valve model given a step up followed by a step down input is given in Fig. 16 as a dashed line. The time responses will be discussed in the following section.

4 An Alternative Model

Root locus plots and nonlinear simulations show advantages to keeping the inlet orifice to the control volume small relative to the outlet orifice. This allows for a small movement in the pilot poppet to establish an exit orifice that is much larger than the inlet orifice and hence a dramatic decline in the pressure of the control volume. This pressure drop in turn provides the desired quick upward movement of the main poppet. In contrast, making the inlet orifice too small can significantly increase the valve's close time. When the solenoid is shut off the spring force will quickly move the pilot poppet and close the exit orifice to the control volume but the main poppet will not close immediately. The spring force is not strong enough to counter the upward force on the main poppet due to supply pressure. The pressure in the control volume must increase enough to force the main poppet closed. This pressure rise rate is dependent on the size of the inlet orifice and hence a reason to moderate its size.

Designing the inlet orifice to accommodate both adequate open and close times for the valve is possible but forces a compromise. An alternative which avoids this compromise is a model that contains a variable inlet orifice to the control volume. As the pilot poppet opens the inlet orifice would be restricted and the opposite would occur when the pilot was closing, hence reducing the time required to open or close the valve. The variable inlet design is achieved by extending the lower end of the pilot poppet to have a portion which covers the passage that carries Q1 in Fig. 1 as the valve opened. The resulting pilot poppet is depicted in Fig. 14. This design would use the lower edge of the pilot poppet to restrict the flow, Q1, into the control volume that is located between the pilot poppet and the main poppet. The restriction orifice area would depend on the pilot poppet position as can be seen in the figure.

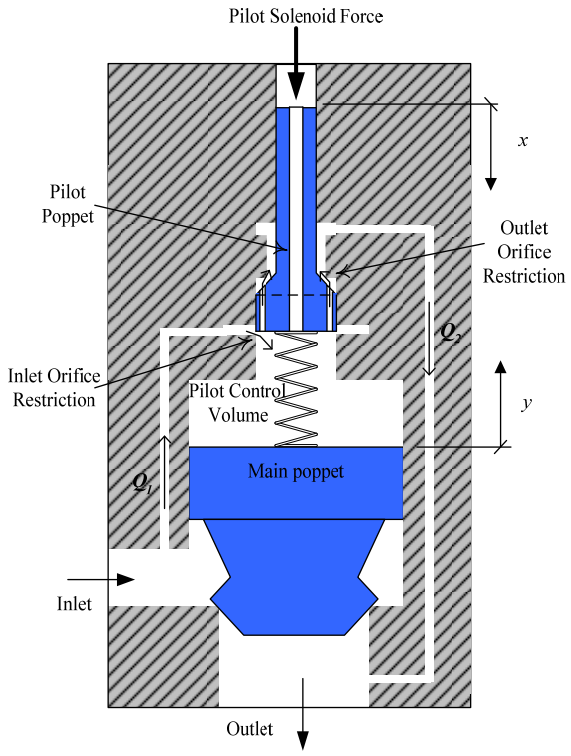

Fig. 14: *Diagram of the alternative valve model*

Slight changes to Eq. 9 and 10 provide the adaptations needed to create a variable inlet orifice to the control volume. Equation 17 is derived from Eq. 9 with two additional terms to account for flow forces due to the variable inlet orifice. Now the pilot poppet controlls the flow through two orifices, the inlet and the outlet. The net flow force due to the inlet orifice tends to open the pilot poppet outlet orifice. At the same time the flow force due to the inlet orifice tends to restrict the inlet orifice due to the direction of the flow force. In Figure 14, there are arrows at the locations labeled inlet orifice restriction and outlet orifice restriction. These arrows give an indication of the directions of the jet angles which relate to flow force directions.

$$m\ddot{x} = -B_x\dot{x} - k(y_n + x_n) - kfq_2 x_n + kfq_1 x_n - kfc_1 P_C - kfc_2 (P_C - P_L) + f + kfc_1 P_s \tag{17}$$

Equation 18 is Eq. 10 with one additional term to account for decreasing flow into the control as the pilot poppet opens. It should be noted that both kq_1 and kfq_1 will be negative due to the negative relationship between x and the area of orifice one, the inlet orifice.

$$\dot{P}_c = \frac{\beta}{V_{CO}} \left\{ \begin{matrix} A_C\dot{y} + kq_1 x_n - kq_2 x_n - kc_1 P_C - \\ kc_2 (P_C - P_L) + kc_1 P_s \end{matrix} \right\} \tag{18}$$

The iterative root locus procedure performed on the first model, to be referred to as the "fixed orifice" model, is also employed to optimize the second model or the "variable orifice" model. Again, the Bode diagram presented is for the optimized system with load pressure held constant and the main poppet position set as the output. Figure 15 shows that the shape of the Bode diagram for the variable orifice model is similar at low frequencies compared to the fixed orifice model but the bandwidths increase as was hoped. The system bandwidth is 85 Hz

for a 35 MPa pressure drop across the valve and 11.87 Hz for a 1 MPa pressure drop. This exceeds the 8 Hz bandwidth established as a performance objective but again more efforts must be made in modeling realistic load dynamics before accepting this number.

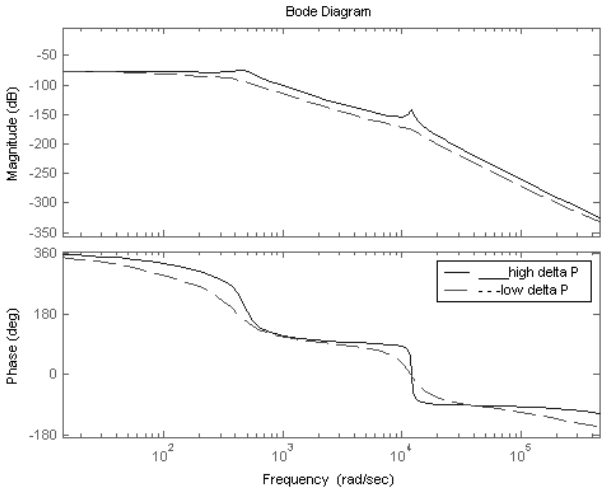

Fig. 15: *Bode diagram for variable orifice model, 0.1 mm opening 35 MPa = high ΔP and 1 MPa = low ΔP*

A greater bandwidth suggests that the variable orifice model will have a faster step response than the constant orifice model. Nonlinear simulations are relied upon to examine how fast the valve will close when the forcing input or solenoid force is shut off. A step input force was given to both nonlinear models in order to open the valve six millimeters but at 0.2 seconds the force was turned off. The system model equations were integrated using a variable step differential equation solver, ODE45, in the Mathworks MATLAB software. Figure 16 displays the position of the main poppet with time, where the supply pressure is 2.1 MPa and the load pressure is 1 MPa.

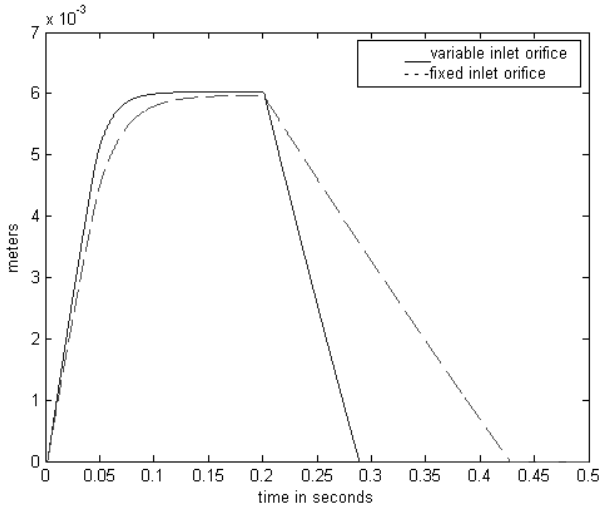

Fig. 16: *Valve position for both models: ΔP = 1 MPa P_S = 2.1 MPa*

It is evident from Fig. 16 that the variable orifice model provides a slightly faster opening and closes in less than half the time of the constant orifice model. It is noted that the above simulation is with a low supply pressure for the purpose of examining the worse case scenario. At higher supply pressures the variable orifice model continues to out perform the constant orifice model but with a decreasing margin.

Conclusions

In conclusion this paper presents dynamic modeling design techniques for a two stage metering poppet valve with a forced feedback configuration. In particular root locus and Bode diagrams provide a systematic method to tune parameters so as to improve valve performance. Evidence suggests that effective damping on the pilot poppet coupled with an appropriately sized feedback spring leads to a stable system. A spring constant which is too small leads to unstable behavior due to interaction with the load dynamics. Appropriate sizing of the inlet orifice to control volume and the slope of the outlet orifice to pilot poppet position relationship provides a means to improving the system bandwidth while limitations are reached at the lowest pressure drops. In general, increasing the inlet orifice size increases system performance since a low frequency pole is moved to a higher frequency as the orifice area is increased. If the inlet orifice is too small, unstable poles can be seen in the root locus plot due to the load dynamics. Also, a small inlet area of the valve leads to slow valve closing times.

Since there is a trade off between fast opening and fast closing in the basic valve design, a new concept was needed. An alternative model where the inlet orifice is allowed to vary was also presented. The variable inlet model analysis shows that higher bandwidth performance can be achieved. Also, the closing time of the valve is improved.

Future work will include an analysis of the frequency response for a range of different valve openings to help understand the effects of nonlinearities on the system dynamics. Although progress has been made towards achieving performance goals, future work must also focus on validation of the design techniques using experimental data. Once experimental validation is completed, work can proceed with modeling more realistic load conditions for the valve. Once the interaction between load dynamics and valve performance is better understood, this work naturally leads into the design of a feedback controller for the purpose of reliably metering flow. The results of this work are being used to build a prototype of the valve design. The valve will be tested to determine if experimental results validate the goals of the modeling and design process.

Nomenclature

A_C	Area of main poppet exposed to control pressure	[m^2]
A_L	Area of main poppet exposed to load pressure	[m^2]
A_S	Area of main poppet exposed to supply pressure	[m^2]
a_1	Area of the orifice from supply to control volume	[m^2]
a_2	Area of the orifice between control and load volumes	[m^2]
a_3	Area of the orifice from supply to load volume	[m^2]
a_4	Area of the orifice from the load volume to tank	[m^2]
b_X	Damping coefficient for the pilot poppet	[N/m/s]
b_Y	Damping coefficient for the main poppet	[N/m/s]
C_d	Orifice discharge coefficient	
f	Actuator input force	[N]
h_2	Slope of orifice 2 area vs. position curve	[m^2/m]
h_3	Slope of orifice 3 area vs. position curve	[m^2/m]
k	Feedback spring coefficient	[N/m]
$kc_{(1-4)}$	Pressure flow coefficient for orifices 1-4	[m^3/s/Pa]
$kfc_{(1-3)}$	Pressure flow force coefficient for orifices 1 - 3	[N/Pa]
$kq_{(1-3)}$	Flow gain for orifices 1 – 3	[m^3/s/m]
M	Mass of the main poppet	[kg]
m	Mass of the pilot poppet	[kg]
o	All *o* subscripts represent nominal conditions	
P_C	Control volume pressure	[Pa]
P_L	Load volume pressure	[Pa]
P_S	Fixed supply pressure	[Pa]
P_T	Fixed tank pressure	[Pa]
$Q_{(1-4)}$	Flow rate across orifices 1 - 4	[m^3/s]
θ	Jet angle for flow force	[rad]
V_C	Volume of the control volume above the main poppet	[m^3]
V_L	Load volume	[m^3]
x	Position of the pilot poppet referenced from closed position (positive is down in Fig. 1)	[m]
x_n	Pilot poppet position referenced from the nominal opening	[m]
y	Position of the main poppet referenced from closed position (positive is up in Fig. 1)	[m]
y_n	Main poppet position referenced from the nominal opening	[m]
β	Fluid bulk modulus	[Pa]
ρ	Fluid density	[kg/m^3]

References

Aardema, J. A. 1997, *Pilot Valve for a Flow Amplyifying Poppet Valve*, U.S. Patent 5 645 263, 1997.

Fales, R. 2006. Stability and Performance Analysis of a Metering Poppet Valve. *International Journal of Fluid Power*. Vol. 7, No. 6, Pages 11-18.

Funk, J. E. 1964. Poppet Valve Stability, *Journal of Basic Engineering*, pp. 207-212**.**

Hayashi, S. 1995. Instability of Poppet Valve Circuit, *JSME International Journal*, Series C, Vol. 38, No. (3), pp. 357-366.

Li, P. Y., 2002, "Dynamic Redesign of a Flow Control Servovalve Using a Pressure Control Pilot," Journal of Dynamic Systems, Measurement, and Control, Vol. 124, pp 428-434.

Manring, N. D. 2005. *Hydraulic Control Systems*, Hoboken, NJ: John Wiley & Sons, pp. 224-228.

Opdenbosch, P., **Sadegh, N.** and **Book, W.** 2004. Modeling and Control of an Electo-hydraulic Poppet Valve. *ASME International Mechanical Engineering Congress and Exposition*, Anaheim, CA.

Schexnayder, L. F. 1995. *Poppet Valve with Force Feedback Control*, U.S. Patent 5 421 545, 1995.

Yang, X., **Paik, M. J.** and **Pfaff, J. L.** 2004. *Pilot Operated Control Valve Having a Poppet With Integral Pressure Compensating Mechanism*, U.S. Patent 6 745 992, 2004.

Yang, X., **Stephenson, D. B.** and **Paik, M. J.** 2005. *Hydraulic Poppet Valve with Force Feedback*, U.S. Patent 6 869 060, 2005.

Zhang, R., **Alleyne**, **A. G.** and **Prasetiawan, E. A.** 2002. Performance Limitations of a Class of Two-Stage Electro-Hydraulic Flow Valves, *International Journal of Fluid Power*, Vol. 3, No. (1).

Matt Muller
Muller received a M. S. in mechanical engineering at the University of Missouri – Columbia in 2006. His graduate work focused on design and control of metering poppet valves. In 2006, Muller joined Caterpillar Inc. with research responsibilities in the area of hydraulic systems.

Roger Fales
Fales received undergraduate and M.S. degrees in Mechanical Engineering at Kansas State University in 1996 and 1998 respectively. He was employed at Caterpillar Inc. from 1998 to 2002 as a research engineer in the area of hydraulic systems and controls. He returned to school at Iowa State University and received a Ph.D. in Mechanical Engineering in 2004. In 2004, he joined the Mechanical & Aerospace Engineering Department at the University of Missouri – Columbia. As an assistant professor, he teaches and does research work in the areas of dynamics, systems, automatic control, and fluid power.